The Hyperfine Structure of the $3P_{3/2}$ State of Na^{23}†

PAUL L. SAGALYN
Research Laboratory of Electronics and Department of Physics, Massachusetts Institute of Technology, Cambridge, Massachusetts
(Received February 9, 1954)

Two of the separations in the hyperfine structure of the $3P_{3/2}$ state of Na^{23} were measured. The results are 61 ± 2 Mc/sec and 36.6 ± 2 Mc/sec. These results were assigned to the $(F=3\leftrightarrow F=2)$ and $(F=2\leftrightarrow F=1)$ separations. A value of $Q=+0.1\pm0.06\times10^{-24}$ cm² was calculated for the nuclear electric quadrupole moment.

I. INTRODUCTION

UP to the present time it has not been possible to measure the nuclear electric quadrupole moments of the alkali metals. In order to use the results of molecular spectroscopy, more accurate molecular wave functions are required than are available at present. Measurements of the hyperfine structure of the $S_{1/2}$ ground state of the sodium atom have been made by the molecular beam method.[1] Jackson and Kuhn[2] made a study of the absorption spectra of a beam of sodium atoms and succeeded in resolving the hyperfine structure of the $3P_{1/2}$ first excited state, but not of the $3P_{3/2}$ state. All S states and also $P_{1/2}$ states give an electric field with zero gradient at the nucleus. Since the interaction energy of the nuclear quadrupole moment with the atomic electrons is proportional to the gradient of the electric field at the nucleus, these measurements yield no information about the quadrupole moment.

We have made a direct measurement of the hyperfine structure of the $3P_{3/2}$ first excited state of sodium by the "double resonance" method.[3,4] From the deviations from the interval rule for hyperfine structure we obtain a value for the quadrupole moment.

II. THE METHOD

The "double-resonance" method, first proposed by Kastler and Brossel,[3] has been discussed in detail by Brossel and Bitter.[5] Atoms are irradiated with their own resonance radiation and raised from the ground state to the first excited state. Since the incident radiation is not isotropic, the populations of the various levels of the excited state will not all be equal. Consider a pair of levels in the excited state whose energy difference is $E=h\nu$, where h is Planck's constant, and ν is a frequency. If an external alternating magnetic field is applied, then, depending on certain selection rules, transitions may occur between the two levels. (The transition probability is a maximum when the frequency of the magnetic field is equal to E/h.) This redistribution of atoms in the excited state may be observed as a change in the spatial intensity distribution of the re-emitted light.

The word "transition" used above should be treated with caution. When the alternating field is applied to an atom, a time-dependent term is added to the Hamiltonian, and the wave functions describing the excited state are no longer eigenfunctions of the Hamiltonian. A complete wave-mechanical theory which takes into account both the spontaneous electric dipole (optical) transitions and the induced magnetic dipole transitions is not yet available. The notion that the alternating field merely causes the atoms to slip back and forth between the unperturbed states appears to work and will be used here.

The structure of the sodium resonance line is shown in Fig. 1. The nuclear spin of sodium[6] is $I=3/2$. The atomic ground state is $3\,^2S_{1/2}$, that is, a doublet S state

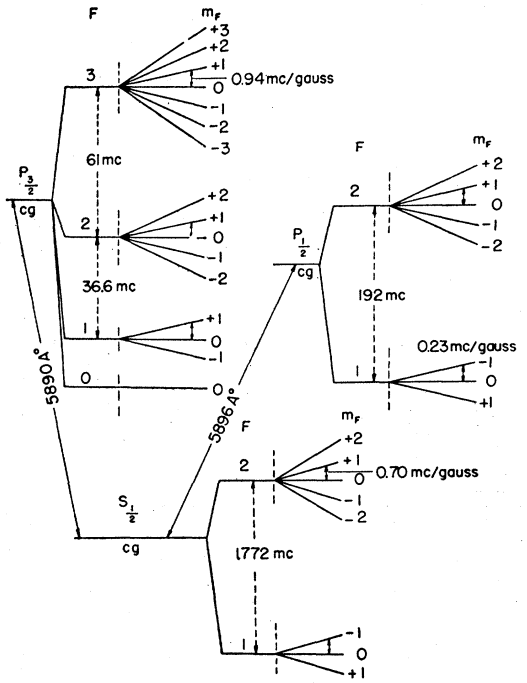

FIG. 1. The sodium resonance lines, not drawn to scale.

† This work was supported in part by the U. S. Signal Corps, the Air Materiel Command, and the U. S. Office of Naval Research.

[1] P. Kusch and H. Taub, Phys. Rev. **75**, 1477 (1949).

[2] D. A. Jackson and H. Kuhn, Proc. Roy. Soc. (London) **167**, 205 (1938).

[3] J. Brossel and A. Kastler, Compt. rend. **229**, 1213 (1949).

[4] I. I. Rabi [Phys. Rev. **87**, 379 (1952)] recently proposed a method of extending molecular beam techniques to excited states. At the time of this writing no results had been published.

[5] J. Brossel and F. Bitter, Phys. Rev. **86**, 308 (1952).

[6] J. E. Mack, Revs. Modern Phys. **22**, 64 (1950).

TABLE I. Hyperfine structure data for the $3P$ levels of sodium.

J state	F values	$E_F-E_{F'}$ calculated Mc/sec	$E_F-E_{F'}$ observed Mc/sec	a calculated Mc/sec
		$Z_i=7.41$		
$P_{1/2}$	2−1	199	192 ±10	99.5
$P_{3/2}$	3−2	59.7	61 ± 2	19.9
	2−1	39.8	36.6± 2	
	1−0	19.9		

with principal quantum number $n=3$ and total electronic angular momentum quantum number $J=1/2$. The two possible values of F, the total angular momentum, are $3/2+1/2=2$, and $3/2-1/2=1$. The hyperfine structure has been measured by molecular beams and is 1772 Mc/sec.[1]

The first excited state of sodium is a doublet consisting of a $3\,^2P_{1/2}$ term and a $3\,^2P_{3/2}$ term. Their separation[7] is 17.18 cm^{-1} or 5.16×10^5 Mc/sec. The $3\,^2P_{1/2}$ state has two hyperfine states corresponding to $F=2$ and $F=1$. The $3\,^2P_{3/2}$ state has four values of F: 3, 2, 1, and 0. The wavelengths of the two resonance lines are 5896A and 5890A, when measured from the center of gravities of the hyperfine structures. The $3\,^2P_{1/2}$ state lies lower and gives the longer wavelength line. The hyperfine separation of the $3\,^2P_{1/2}$ state is $(6.4\pm0.3)\times10^{-3}$ cm^{-1}, or 192 Mc/sec.[2,8–10]

As an experimental guide the hyperfine separation may be calculated from a formula for the magnetic interaction constant derived by Goudsmit.[11] The results are tabulated in Table I. This formula neglects the quadrupole interaction. The magnetic interaction constant is, from the Goudsmit formula,

$$a=\frac{g_I}{1836}\frac{\Delta\nu L(L+1)}{Z_i(L+1/2)J(J+1)}\frac{k}{\lambda}, \tag{1}$$

where L is the orbital electronic angular momentum quantum number, J is the total electronic angular momentum quantum number, g_I is the nuclear g factor, $\Delta\nu$ is the fine structure separation, Z_i is the inner atomic number, and k/λ is a relativistic correction. The shift in energy of a term with a given value of F, measured from the center of gravity of the line, is given by $E_F=a/2[F(F+1)-I(I+1)-J(J+1)]$. The value used for Z_i was 7.41 as calculated from the following equation due to Casimir:[12]

$$\Delta\nu=\frac{dn^*}{dn}Z_i^2\frac{R}{n^{*3}L(L+1)}\alpha^2. \tag{2}$$

n^* is the effective quantum number, n the principle quantum number, and α is the fine structure constant. n^* is determined by E_n, the term value of the doublet center of gravity:

$$E_n=-R/n^{*2}, \tag{3}$$

where R is the Rydberg.

In Table II are tabulated the g factors and splitting factors in (Mc/sec) per gauss for all the levels involved in the sodium resonance line, for a very weak, steady magnetic field, that is, a field which does not decouple I and J.

The values tabulated are calculated from the formulas

$$g_F\approx g_J\frac{F(F+1)+J(J+1)-I(I+1)}{2F(F+1)},$$
$$g_J=1+\frac{J(J+1)+S(S+1)-L(L+1)}{2J(J+1)}, \tag{4}$$

and $-\Delta T_F=g_F M_F(He)/(4\pi mc)$, where M_F represents the projection of F along the magnetic field, H is the magnitude of the steady magnetic field, e is the electronic charge, m the electronic mass, c the velocity of light, and ΔT_F is the shift in the term value of the field free state. Therefore, a positive ΔT_F means that the energy of the level decreases.

The complete Zeeman diagram for $J=3/2$ and $I=3/2$ out to fields large enough to decouple I and J is found in a paper by Davis, Feld, Zabel, and Zacharias.[13] This diagram is reprinted in Fig. 2.

The limit to the accuracy with which the separations can be measured is set by the natural linewidths of the levels. The lifetime τ_n of the P state is known[14] to be 1.48×10^{-8} sec. Then the "half-widths" of the levels are

TABLE II. Zeeman effect data for the states involved in the sodium resonance lines.

J state	F level	g_F	$\lvert T_F/M_F H\rvert$ (Mc/sec) per gauss
$P_{1/2}$	2	1/6	0.234
	1	−1/6	0.234
$P_{3/2}$	3, 2, 1, 0	2/3	0.935
$S_{1/2}$	2	1/2	0.70
	1	−1/2	0.70

[7] H. E. White, *Introduction to Atomic Spectra* (McGraw-Hill Book Company, Inc., New York, 1934), Table 17.5.

[8] An early attempt to measure the hyperfine structure of the $3\,^2P_{3/2}$ state was made by Ellett and Heydenburg (reference 9) and by Larrick (reference 10). Their method consists of measuring the depolarization of the resonance radiation by small magnetic fields, and then fitting the data to a theoretical curve in which the hyperfine structure constant appears as a parameter. The results do not agree well and, moreover, it is necessary in the theory to assume a pure magnetic interaction.

[9] A. Ellett and N. P. Heydenburg, Phys. Rev. **46**, 583 (1934).

[10] L. Larrick, Phys. Rev. **46**, 581 (1934).

[11] S. Goudsmit, Phys. Rev. **43**, 636 (1933).

[12] H. B. G. Casimir, *On the Interaction Between Atomic Nuclei and Electrons* (Teylers Tweede Genootschap, Haarlem, 1936), Eq. (14, 4), p. 54.

[13] Davis, Feld, Zabel, and Zacharias, Phys. Rev. **76**, 1076 (1949).

[14] R. Ladenberg and E. Thiele, Z. Physik **72**, 697 (1931).

given by the expression

$$\Delta\nu_n = 1/(2\pi\tau_n), \quad (5)$$

or 10.7 Mc/sec in the case of sodium. If the transition probability for the radiofrequency is small compared with the optical transition probability, we may expect that the minimum radio-frequency transition width will be approximately 21 Mc/sec.

The amplitude needed for the radio-frequency field can be estimated from the equation for the transition probability by means of perturbation theory:[15]

$$h^2P(FM_F:F'M_F') = \pi^2t^2\mu_0^2g_J^2 \times|(F,M_F|J_xH_x'+J_yH_y'+J_zH_z'|F',M_F')|^2, \quad (6)$$

where t is the time spend by the atom in the oscillating field, μ_0 is the Bohr Magneton, and the expression in parenthesis is the matrix element of the perturbation between levels characterized by quantum numbers F, M_F, and F', M_F', respectively. In this experiment the oscillating field had a component in only one direction. The matrix elements are given in reference 13. If we take 20 as a rough average for the matrix element, t as the lifetime of the state, and $P=0.1$, then $H'=5$ gauss.

III. APPARATUS

A schematic drawing of the experiment is shown in Fig. 3. A standard Cenco sodium arc is placed on the x axis. The collimating lens and polaroid form a beam of plane polarized light which illuminates the front face of the resonance lamp. Two beams of scattered light are taken from the resonance lamp. The horizontal

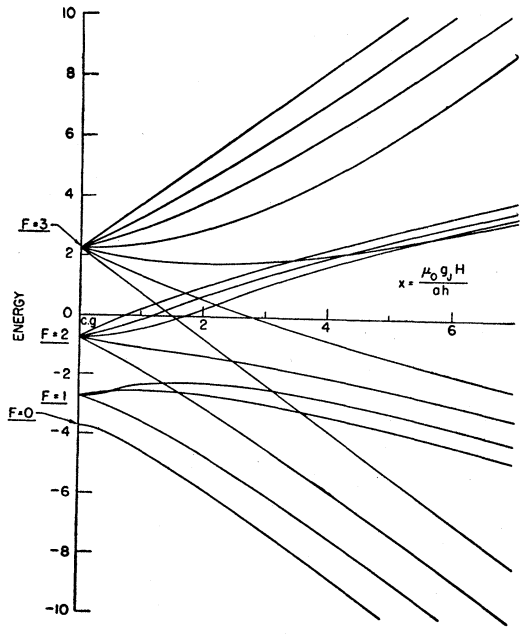

FIG. 2. Theoretical energy level diagram for state with $I=J=3/2$, neglecting the quadrupole interaction.

[15] I. I. Rabi, Phys. Rev. 51, 652 (1937).

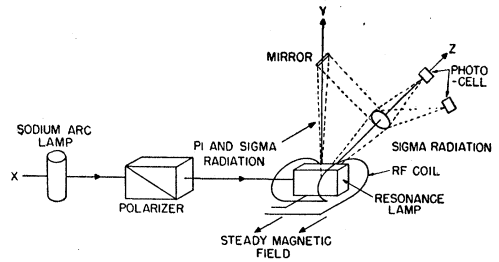

FIG. 3. Schematic drawing of the apparatus.

beam passes directly through the lens on the z axis and hits one photomultiplier. The vertical beam hits a small mirror on the y axis and then passes through the same lens to another photomultiplier. We used 1P21 multipliers because of their high sensitivity in the yellow region. Both phototubes are in the $y-z$ plane. The output currents of the two multipliers are combined in a simple bridge circuit similar to the one shown in Fig. 4 of reference 5. Two galvanometers are used. One is in series with the horizontal beam tube and monitors the full current independent of the beam balance. The body of the resonance lamp is made out of precision square-bore Pyrex tubing made by Fisher Porter Company. The inside surface of this tubing is accurately plane, and when the outside was polished, the walls made very acceptable windows for the re-emitted light. A Pyrex window was sealed on the front of the body and a horn on the back. Sodium is distilled into the lamp under high vacuum. Glow discharges started by the radio-frequency caused considerable trouble in the early cells. Care must be taken to seal off at a pressure well below 10^{-6} mm. The resonance lamp is located inside a water-cooled coil consisting of four turns, each 2 in. in diameter, wound from $\frac{3}{16}$-in copper tubing. The whole assembly is placed inside a simple oven. The resistance of the coil could be measured with the Q meter, and was 0.65 ohms at 36 Mc/sec and approximately 2 ohms at 60 Mc/sec. The power required, theoretically, for $H=5$ gauss was 40 watts at 36 Mc/sec, and 100 watts at 60 Mc/sec. The range of power actually used was 60 to 80 watts.

The output of the rf power amplifier was taken out through a flexible cable and link coupled to the coil in the oven. By tuning the coil and varying the coupling it was possible to match the line impedance. For this purpose a micromatch unit manufactured by the M. C. Jones Company proved valuable. This device reads incident and reflected power separately. With an incident power of 60 watts it was always possible to reduce the reflected power below 1 watt and to monitor the absorbed power to better than ± 2 watts.

IV. DISCUSSION OF RESULTS

Two types of data were taken: (a) curves of signal *vs* radio-frequency in zero (i.e., the earth's) magnetic field, and (b) curves of signal *vs* magnetic field for con-

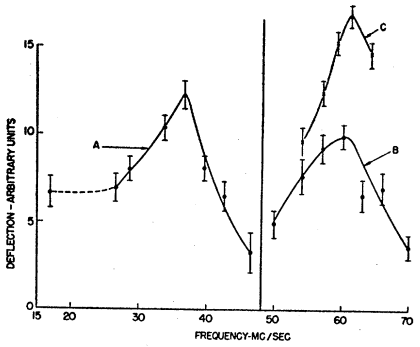

FIG. 4. Experimental resonance curves in zero field. The deflection caused by turning the radio-frequency on and off is plotted *vs* the frequency.

stant radiofrequency. The quantitative data on the hyperfine structure is obtained from the first set of data. These will be discussed first. It has only been possible to give a partial qualitative explanation of the second set of data.

(a) The signal *vs* frequency data is plotted in Fig. 4. Only one point was taken below 26 Mc/sec because of the difficulty in tuning the present equipment. Curve C contains the results of a successful attempt to obtain the high-frequency maximum with greater precision.

We take the position of the highest frequency maximum to be $E=61\pm2$ Mc/sec, and the position of the next to be $E'=36.6\pm2$ Mc/sec.

We now identify each of these frequencies with one of the separations in the $P_{3/2}$ state. In support of this we note that the half-width is approximately correct and that the frequencies are close to two of the values previously given by the Goudsmit formula. Also the known separations of the $P_{1/2}$ and $S_{1/2}$ states are much larger than either of these values.

The question now is, to which of the separations in the $P_{3/2}$ state do the experimental values E and E' correspond? Let $E_{FF'}$ denote the separation between levels characterized by F and F'. Then the separations satisfy equations of the form:[13]

$$\begin{aligned} E_{32}&=3a_{3/2}+b,\\ E_{21}&=2a_{3/2}-b,\\ E_{10}&=a_{3/2}-b. \end{aligned} \tag{7}$$

Here $a_{3/2}$ is the magnetic interaction in the $P_{3/2}$ state; it corresponds to setting $J=3/2$ in Eq. (1). The quantity b is the electric quadrupole interaction which is proportional to Q, the nuclear electric quadrupole moment.

There are six possible correlations of Eqs. (7) with the experimental data: (1) $E_{32}=61$, $E_{21}=36.6$; (2) $E_{32}=36.6$, $E_{21}=61$; (3) $E_{21}=61$, $E_{10}=36.6$; (4) $E_{10}=61$, $E_{21}=36.6$; (5) $E_{32}=61$, $E_{10}=36.6$; (6) $E_{10}=61$, $E_{32}=36.6$. If we use Eqs. (7) we obtain 19.5 ± 0.6 Mc/sec for the magnitude of a in cases (1) and (2) and 24.4 ± 2.8 in the other four cases.

Cases (3) through (6) can be eliminated by the following considerations. The theory of atomic structure yields expressions for the magnetic hyperfine structure interactions and the fine structure interaction which are independent of the nuclear electric interaction and can be written in the following way:

$$\langle r^{-3}\rangle_1=\frac{J(J+1)}{L(L+1)}\frac{1}{2\mu_0^2}\frac{1}{g_I/1836}ha_{1/2}, \tag{8a}$$

$$\langle r^{-3}\rangle_2=\frac{J(J+1)}{L(L+1)}\frac{1}{2\mu_0^2}\frac{1}{g_I/1836}ha_{3/2}, \tag{8b}$$

$$\langle r^{-3}\rangle_3=\frac{\Delta\nu}{\mu_0^2(2L+1)Z_i}. \tag{8c}$$

Each of the magnetic interactions is proportional to the average value of r^{-3}. The three values of $\langle r^{-3}\rangle$ are qualitatively the same but are not identical. Equation (1) which was used to calculate the values listed in Table I is based essentially on the assumed equality of these expressions.

If we set (8b) equal to (8c) then we obtain (see Table I) $a_{3/2}=19.9$ Mc/sec. We consider the experimental error in $\Delta\nu$ to be negligible for our purposes. We might also equate (8a) and (8b). This gives $a_{3/2}=19.2\pm0.9$. Here we have taken into account the experimental error in $a_{1/2}$. To each of these numbers should be attached an additional error to take into account the differences in $\langle r^{-3}\rangle$. This problem has been investigated theoretically by Koster.[16] It was shown that in aluminum the three equations agree within 1.5 percent. Aluminum has a $3s^23p$ configuration, that is, one electron outside a closed subshell. Sodium has one p electron outside a closed shell. This makes the one electron approximation even better for sodium. Sodium has a lower Z which should also help. However, it is difficult to estimate the error involved in using Eq. (8c) precisely because of the uncertainty in Z_i. Equation (8c) is actually the definition of the Z_i, but Eq. (2) which was used for calculating Z_i is approximate. We may conclude, however, that the theory is good enough to enable us to eliminate cases (3) through (6) above on the grounds that they give wrong values for $a_{3/2}$.

Case (2) predicts the correct value for $a_{3/2}$ but predicts 41.5 Mc/sec for the E_{10} transition. There is no sign of this transition in the zero-field data. Case (1) predicts 17.1 Mc/sec for the E_{10} transition. Because of tuning difficulties only one point was obtained in this region. The asymmetry of curve (a) in Fig. 4 and the one point that was taken seem to indicate the presence of this transition. We therefore take case (1) to be correct. The values of $a_{3/2}$ and b computed from the data obtained in this experiment are then

$$\begin{aligned} a_{3/2}&=19.5\pm0.6 \text{ Mc/sec},\\ b&=\ 2.4\pm1.4 \text{ Mc/sec}. \end{aligned} \tag{9}$$

[16] G. F. Koster, Phys. Rev. **86**, 148 (1952).

The magnetic interaction in E_{32} is just $3a_{3/2}$. If we compute this using the value of $a_{3/2}$ obtained from $\Delta\nu$ and then subtract from our value for E_{32}, we obtain $b=1.3 \pm 2.1$ Mc/sec. Z_i was assumed here to be uncertain to 1 percent. Doing the same but using $a_{1/2}$, gives $b=3.3 \pm 3.4$ Mc/sec. These numbers are not in disagreement with Eq. (9), but because of the actual uncertainty in Z_i and the rather large probable errors here, we take Eqs. (9) as representing our best values for $a_{3/2}$ and b.

It should be emphasized at this point, that, for lack of a theory, we have not taken into account the possibility that, because of the presence of the rf field, the position of the maximum of the curve may not correspond exactly to the energy of the isolated atom. However, as pointed out in the section on signal intensities, the rf transition probability was much smaller than the optical transition probability. Under these circumstances the effect of the rf can probably be neglected.

The quadrupole moment of the nucleus is defined by the expression

$$eQ=\int (3z^2-r^2)\rho_n d\tau, \tag{10}$$

where ρ_n is the nuclear charge density. The averaging is to be done in the state in which $M_I=I$. In reference 13 it is shown that if the electronic wave function is assumed to be separable, the following relationship exists between Q and b:

$$hb=e^2Q\frac{2L}{2L+3}\langle r^{-3}\rangle, \tag{11}$$

where $\langle r^{-3}\rangle$ indicates an average over the electronic state in which $M_J=J$. L is the orbital electronic quantum number. Any part of Eq. (8) may now be used to compute Q with sufficient precision:

$$Q=0.041b \text{ cm}^2\times 10^{-24}, \tag{12}$$

where b is expressed in Mc/sec.

From (9) we obtain

$$Q=(0.1\pm 0.06)\times 10^{-24} \text{ cm}^2. \tag{13}$$

We have not included here any corrections of the type considered by Sternheimer.[17] If case (2) had been taken as the correct interpretation of the data, the value obtained for Q would have been -2.3×10^{-24} cm^2. This would seem unreasonably large in magnitude for a light nucleus.

(b) It is more difficult to account for the data taken by measuring the radio-frequency deflection as a function of the steady magnetic field at various frequencies.

In Fig. 5 are shown most of the possible radio-frequency transitions. These curves were taken from the data used to plot Fig. 1 of reference 13. The transitions left out have very small matrix elements.

Representative samples of the experimental results are shown in Figs. 6 and 7. The experimental curves all appear to be the sum of two curves of the resonance type although the shape of the curves is quite different at different frequencies. The position of the low-field maximum has been plotted as a function of the frequency, shown by dots plotted on the right side of Fig. 8. The crosses are the estimated positions of the high field maximums plotted as a function of frequency. Consider the circles. We can convert any of the theoretical curves of transition frequency *versus* x, Fig. 5, into Mc/sec and gauss by assuming a value for the zero-field separation. For example, if we choose $a=17$ and $1=17$ Mc/sec on the frequency scale, then $H=9.1x$ gauss. The theoretical curves actually neglect the quadrupole interaction. To first order we may assume that the effect of the quadrupole interaction is to change the zero field separation without affecting the shape of the curves. For a frequency of 80.2 Mc/sec, the highest that was used, varying the magnetic field

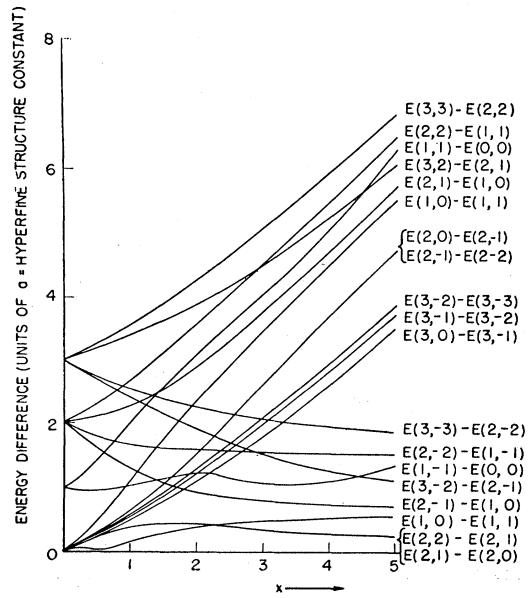

FIG. 5. Theoretical rf transition frequencies in units of a *versus* x.

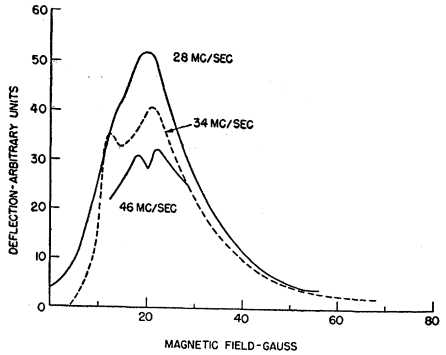

FIG. 6. Experimental resonance curves at constant frequency. The deflection caused by turning the radio-frequency on and off is plotted *vs* the magnetic field, for various frequencies.

[17] R. Sternheimer, Phys. Rev. **80**, 102 (1950).

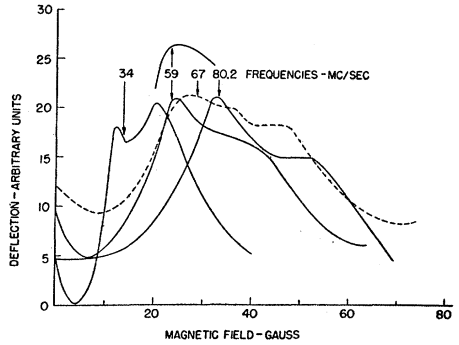

FIG. 7. Experimental resonance curves at constant frequency. The deflection caused by turning the radio-frequency on and off is plotted *vs* the magnetic field, for various frequencies.

moves us horizontally along the 4.7 line in Fig. 5. Two major groups of transitions appear, one centered roughly about $E(11)-E(00)$ and the other centered about $E(3-1)-E(3-2)$. These two transitions have been plotted in Fig. 8 for $a=17$. This value of a was chosen as giving the best agreement at the higher frequencies where the situation is simplest. Accurate correlation with the zero field data cannot be expected because of the overlapping of transitions caused by the large level widths. The most satisfactory feature of this data is that the sharp cutoff of the signal at the high end of the magnetic field scale (Figs. 6, 7) is in agreement with the theoretical curves. At low fields and frequencies the situation becomes very complicated.

A puzzling feature of the curves is the minimum in the signal which always occurs in the region between 0–10 gauss. It is probably significant that this is the region in which the degeneracy is being removed by the steady magnetic field. From Table II we see that a field of 11 gauss will separate two levels by an amount equal to a level width.

V. SIGNAL INTENSITIES

To calculate the effect of the radio-frequency on the scattered light, we start with the radio-frequency off and calculate the populations of the various excited states for a given type of optical excitation in the presence of a weak magnetic field. "Weak" here indicates a field strong enough to remove the degeneracy in the excited state but not strong enough to decouple I and J. The optical transition probabilities have been derived by Van Vleck.[18] Knowing the populations of the excited states we can calculate the relative proportions of π and σ radiation in the re-emitted light. An upper limit to the effect is found by recalculating the π and σ radiation on the assumption that the radiofrequency equalizes the population of certain pairs of levels, subject to the selection rules $\Delta F=0, \pm1$, $\Delta M_F=0, \pm1$. The oscillating field was actually always perpendicular to the steady field, which restricted the radio-frequency transitions to $\Delta M_F=\pm1$. For π optical excitation, the results were:

$(F+1)-F$	Signal (percent)
3−2	4
2−1	2
1−0	1

The deflections caused by turning off the radio-frequency were measured by a galvanometer and bridge circuit arranged in such a way as to measure the sum of the current changes of the two photomultipliers. This deflection, divided by the total current of one of the photomultipliers, represents the percentage signal. The case of π excitation holds down to zero field.[19]

In practice, the signals at 36.6 Mc/sec and 61 Mc/sec were about the same order of magnitude with 60 watts, and equal to approximately 0.1 percent.

In computing the radio-frequency signals three assumptions were made: (1) The intensity of the exciting optical radiation is independent of frequency; (2) there are no depolarizing collisions; (3) the incident light is perfectly polarized. The degree to which the first two of these assumptions are satisfied may vary from run to run. The maximum interval that could be covered in one run was 10 Mc/sec. Different runs were normalized at a common frequency. In the case of curves (a) and (b) in Fig. 4, the closest points taken are too far apart to permit an accurate normalization. The amplitude of the rf field was monitored by measuring the power absorbed by the coil and correcting for the resistance of the coil, as measured on the Q-meter. The transition

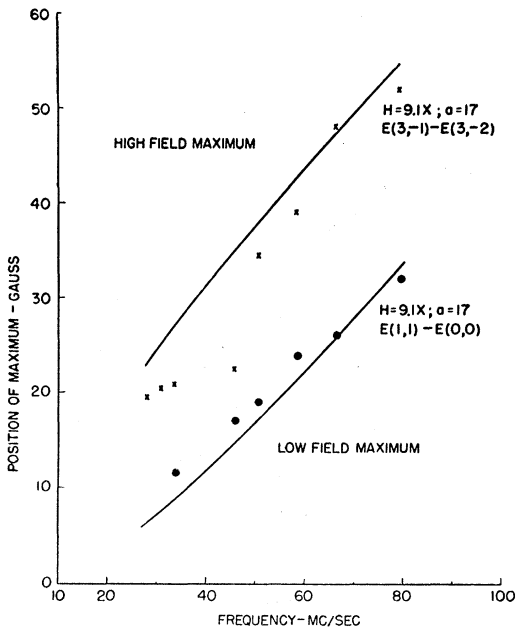

FIG. 8. The values of the magnetic field at which the two principal maxima in Figs. 7 and 8 occur is plotted *vs* the frequency.

[18] J. H. Van Vleck, *Quantum Principles and Line Spectra* (Bulletin of the National Research Council, No. 54, vol. 10, 1926).

[19] W. Heisenberg, Z. Physik **31**, 617 (1925).

probability is proportional to $(H')^2$, and, therefore, to the current squared, or to the power divided by the resistance. The resistance of the coil was 0.65 ohm at 37 Mc/sec, and roughly 2 ohms at 61 Mc/sec. Therefore for equal amplitude of the radio-frequency field, the 61-Mc/sec signal would be about three times as large as compared with the previously estimated factor of two. The 17-Mc/sec point appears to be about one-half as high as the 36.6-Mc/sec point as expected. We must conclude, however, that the intensity calculations are too crude to be of much use in identifying the transitions.

The experimental signal strength at 61 Mc/sec corresponds to a transition probability of 1/80. With 60 watts we should have obtained about 1/20, with a coil of the dimensions and resistances used. The degree of polarization of the incident light is very important here. In zero field, rotating the plane of polarization of the incident light by 90° is just equivalent to interchanging the photomultipliers and must therefore change the sign of the signal (as it does). Depolarizing collisions will also reduce the absolute value of the signal. In Fig. 9 is shown one run at 28 Mc/sec of signal *vs* radio-frequency power, demonstrating that the dependence is linear.

To improve the signal-to-noise ratio we must increase the radio-frequency power and the light intensity. The former was limited by a glow in the resonance lamp and arcing in the tuning condensers. It should be possible to design a much better light source, since it was discovered after most of the data was taken that the Cenco sodium arc is badly self-reversed.

VI. CORRELATION WITH SHELL MODEL

The quadrupole moment of any one particle system is given by an expression of the form[20]

$$Q=-\frac{2j-1}{2j+2}\langle R^2\rangle_{\text{Av}}. \tag{14}$$

$\langle R^2\rangle_{\text{Av}}$ is the average of the square of the radial extension of the wave function, and j is the total angular momentum of the system. On a one-particle model, the quadrupole moment should therefore always be negative or zero. Mayer[21] has pointed out that on the basis of the extreme shell model, the nuclear spin of Na^{23} is also anomalous. Mayer suggested that the configuration of the ground state of the sodium nucleus may actually be $(d_{5/2})^3$ with the $j-j$ coupling giving a resultant spin, $I=3/2$. The magnetic moment computed on the basis of this model is found to lie appreciably closer to the experimental value than do either of the Schmidt lines.

We have attempted to find additional evidence for the sodium configuration by computing the sign of the nuclear quadrupole moment on the basis of the configuration proposed by Mayer, assuming a central field approximation. We use the method of Gray and Wills.[22]

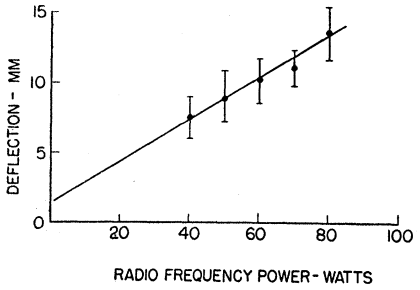

FIG. 9. Radio-frequency deflection *vs* transmitter power.

In a d state, the orbital angular momentum quantum number is $l=2$. Therefore the ten possible one-particle, strong field wave functions are: $u_2^{\pm}u_1^{\pm}u_0^{\pm}u_{-1}^{\pm}u_{-2}^{\pm}$. The plus as a superscript signifies an orbital wave function with spin up, the minus with spin down. The subscripts give the possible values of m_l. First we find the weak field, one-particle wave functions, $\psi[jm]$ where $j=5/2$, as linear combinations of the strong field functions. Since the operator $J_z=L_z+S_z$ has eigenvalues in both representations, we can write at once $\psi[(5/2)(5/2)]=u_{+2}^{+}$. The other five wave functions of the type $\psi[(5/2)m]$ can be found by application of the operators $J_x\pm iJ_y=(L_x+S_x)\pm i(L_y+S_y)$, where

$$(J_x\pm iJ_y)\psi[jm]=\hbar[(j\mp m)(j\pm m+1)]^{1/2}\psi[jm\pm 1]; \tag{15}$$

with similar equations for L_x+iL_y and S_x+iS_y. The results are

$$\begin{aligned}
&\psi[(5/2)(5/2)]=u_2^{+},\\
&\psi[(5/2)(3/2)]=5^{-1/2}\{2u_1^{+}+u_2^{-}\},\\
&\psi[(5/2)(1/2)]=10^{-1/2}\{6^{1/2}u_0^{+}+2u_1^{-}\}\\
&\psi[(5/2)(-1/2)]=10^{-1/2}\{6^{1/2}u_0^{-}+2u_{-1}^{+}\}\\
&\psi[(5/2)(-3/2)]=5^{-1/2}\{2u_{-1}^{-}+u_{-2}^{+}\}\\
&\psi[(5/2)(-5/2)]=u_{-2}^{-}.
\end{aligned} \tag{16}$$

The wave functions of the type $\psi[(3/2)m]$ could be found by finding a linear combination of u_1^{+} and u_2^{-} which is normal and also orthogonal to $\psi[(5/2)(3/2)]$, but these wave functions will not be needed in the present discussion.

Let $\phi(IM_I)$ represent a strong field wave function for the entire system, where $M_I=m_{j1}+m_{j2}+m_{j3}$. The values of I allowed by the Pauli exclusion principle are 3/2, 5/2, 9/2.[23] Consider the state $\phi[(9/2)\times(9/2)]$, that is, the state with the maximum value of M_I. The only possible set of values of m_j, all of which are different, is $[(5/2)(3/2)(1/2)]$. Then the correct antisymmetric linear combination of the one-particle

[20] J. A. Blatt and V. F. Weisskopf, *Theoretical Nuclear Physics* (John Wiley and Sons, New York, 1952).
[21] M. G. Mayer, Phys. Rev. **78**, 16 (1950).
[22] N. M. Gray and L. A. Wills, Phys. Rev. **38**, 248 (1931).
[23] E. U. Condon and G. H. Shortley, *Theory of Atomic Spectra* (Cambridge University Press, London, 1951), Table 2^{10}, p. 263.

wave functions can be written in the usual way as the determinant:

$$\phi[(9/2)(9/2)]=(3!)^{-1/2}\begin{vmatrix}\psi[(5/2)(5/2)]^{(1)} & \psi[(5/2)(5/2)]^{(2)} & \psi[(5/2)(5/2)]^{(3)}\\ \psi[(5/2)(3/2)]^{(1)} & \psi[(5/2)(3/2)]^{(2)} & \psi[(5/2)(3/2)]^{(3)}\\ \psi[(5/2)(1/2)]^{(1)} & \psi[(5/2)(1/2)]^{(2)} & \psi[(5/2)(1/2)]^{(3)}\end{vmatrix}, \tag{17}$$

where the superscripts stand for the particle number. For simplicity, we abbreviate this as

$$\phi[(9/2)(9/2)]=(3!)^{-1/2}\begin{vmatrix}5/2\\ 3/2\\ 1/2\end{vmatrix}, \tag{18}$$

it being understood that this stands for a three-by-three determinant, the numbers given representing the possible values of the m_j. The remaining wave functions of the type $\phi[(9/2)(M_I)]$ can be generated by applying the operator $I_x \pm iI_y$. The result for $\phi[(9/2)(5/2)]$ is

$$\phi[(9/2)(5/2)]=12^{-1/2}\left\{\begin{vmatrix}5/2\\ 1/2\\ -1/2\end{vmatrix}+\begin{vmatrix}5/2\\ 3/2\\ -3/2\end{vmatrix}\right\}. \tag{19}$$

By inspection, we set

$$\phi[(5/2)(5/2)]=12^{-1/2}\left\{\begin{vmatrix}5/2\\ 1/2\\ -1/2\end{vmatrix}-\begin{vmatrix}5/2\\ 3/2\\ -3/2\end{vmatrix}\right\}. \tag{20}$$

We note as proof here that each of the determinants represents a possible strong-field eigenfunction of the system. Therefore each determinant is part of an orthonormal set of wave functions, and therefore $\phi[(9/2)(5/2)]$ is orthogonal to $\phi[(5/2)(5/2)]$. Since there is no other state with $M_I=5/2$, this assignment is unique. We may also generate

$$\phi[(9/2)(3/2)]=(252)^{-1/2}\left\{5^{1/2}\begin{vmatrix}3/2\\ 1/2\\ -1/2\end{vmatrix}+4(2^{1/2})\begin{vmatrix}5/2\\ 1/2\\ -3/2\end{vmatrix}+5^{1/2}\begin{vmatrix}5/2\\ 3/2\\ -5/2\end{vmatrix}\right\}, \tag{21}$$

and

$$\phi[(5/2)(3/2)]=2^{-1/2}\left\{\begin{vmatrix}3/2\\ 1/2\\ -1/2\end{vmatrix}-\begin{vmatrix}5/2\\ 3/2\\ -5/2\end{vmatrix}\right\}. \tag{22}$$

Again, by inspection, we find

$$\phi[(3/2)(3/2)]=2/(63)^{1/2}\left\{-\begin{vmatrix}3/2\\ 1/2\\ -1/2\end{vmatrix}+1/4(10)^{1/2}\begin{vmatrix}5/2\\ 1/2\\ -3/2\end{vmatrix}-\begin{vmatrix}5/2\\ 3/2\\ -5/2\end{vmatrix}\right\}, \tag{23}$$

using the condition that $\phi[(3/2)(3/2)]$ be orthogonal to $\phi[(5/2)(3/2)]$ and $\phi[(9/2)(3/2)]$.

If P_i is the probability of finding the ith proton in the volume element dV at (x,y,z), then

$$P_i(xyz)=\int|\phi|^2 dV_1\cdots dV_{i-1}dV_{i+1}\cdots dV_Z, \tag{24}$$

and we may write

$$\rho_n(xyz)=e\sum_{i=1}^{Z}P_i. \tag{25}$$

Using Eq. (10), the quadrupole moment may then be written as

$$Q=\sum_{i=1}^{Z}\int(3z_i^2-r_i^2)|\phi|^2 d\tau, \tag{26}$$

where now the integration is taken over all the coordinates of all the particles. If we assume that in sodium the first eight protons go into a closed shell with spherical symmetry, then the summation will extend only over the three $d_{5/2}$ particles. The integration involves only elementary integrals and the result is identically zero. It would thus appear that the $(d_{5/2})^3$ configuration cannot account for the sodium quadrupole moment.

ACKNOWLEDGMENT

The author wishes to acknowledge the valuable guidance of Professor Francis Bitter, Department of Physics, Massachusetts Institute of Technology. He is also indebted to Dr. Jean Brossel and Professor I. I. Rabi for their helpful discussions. The financial assistance of a U. S. Atomic Energy Commission pre-doctoral fellowship is also gratefully acknowledged.